Polymer 50 (2009) 5094–5102

Contents lists available at ScienceDirect

Polymer

journal homepage: www.elsevier.com/locate/polymer

Thermal degradation kinetics and mechanisms of PMEPP and MEPP/MMA copolymer

Wan-Jung Chou [a], Guo-An Wang [a], Cheng-Chien Wang [b], Chuh-Yung Chen [a,*], Jen-Lien Lin [c], Shu-Jiuan Huang [c]

[a] Department of Chemical Engineering, National Cheng-Kung University, Tainan 70101, Taiwan
[b] Department of Chemical and Materials Engineering, Southern Taiwan University of Technology, Tainan 710, Taiwan
[c] Material and Chemical Research Laboratories, Industrial Technology Research Institute, Hsinchu, Taiwan

ARTICLE INFO

Article history:
Received 30 April 2009
Received in revised form
16 August 2009
Accepted 27 August 2009
Available online 1 September 2009

Keywords:
2-Methacryloxyethyl phenyl phosphate
Poly(methyl methacrylate)
Thermal degradation

ABSTRACT

In this study, 2-methacryloxyethyl phenyl phosphate (MEPP), a phosphorus-containing flame retardant, was synthesised via the esterification of phenyl dichlorophosphate (PDCP) with 2-hydroxyethyl ethylene methacrylate (HEMA), followed by hydrolysis. A two-stage bulk polymerisation process prepared MEPP/methyl methacrylate (MEPP/MMA) copolymers containing various amounts of MEPP. The condensed-phase and volatized products produced at various temperatures during the thermal degradation of MEPP/MMA copolymer were monitored by Fourier transform infrared (FT-IR) spectroscopy and thermogravimetric analysis with Fourier transform infrared spectroscopy (TGA/FT-IR). Finally, we propose the possible mechanisms for the thermal degradation of MEPP/MMA copolymer according to the analytical results of the condensed-phase and volatilized products.

1. Introduction

Poly(methyl methacrylate) (PMMA) is an important thermoplastic material due to its high optical transmissibility and high weather ability. Therefore, it is widely used in several industries, such as building construction, moulding, and decorative panelling. Unfortunately, PMMA is a highly flammable plastic and is thus limited in many applications. Under normal circumstances, the thermal degradation of PMMA proceeds via the depolymerisation of the methyl methacrylate (MMA) unit, resulting in flammable MMA gas [1–4], which accelerates the burning rate of PMMA. Therefore, the fire resistance and thermal stability of PMMA must be improved in order to increase its commercial value. The fire resistance of PMMA can be improved by the incorporation of flame retardants, such as inorganic materials [5,6], phosphorus-containing compounds [7–12] and halogen-containing compounds [13]. Phosphorous-containing compounds can prevent the release of toxic gases into the atmosphere by acting via a condensed-phase flame-retardant mechanism during burning. This produces a largely incombustible char residue and releases gases that are less toxic than the halogen-containing compounds. Therefore, recent flame retardant technology has focused on phosphorus-containing compounds, which are used to achieve non-toxic PMMA flame retardation with good compatibility between PMMA and flame retardants.

The first use of the reactive phosphorus-containing flame retardant 2-methacryloxyethyl phenyl phosphate (MEPP) in forming an MEPP/methyl methacrylate (MEPP/MMA) copolymer, synthesised by the bulk polymerisation of MMA in the presence of MEPP, has been reported [14]. Additionally, thermogravimetric analysis (TGA) revealed that the incorporation of MEPP into MEPP/MMA copolymers greatly enhanced the thermal stability and amount of char residue. In this report, we discuss the mechanism of the MEPP/MMA copolymer by Fourier transform infrared (FT-IR) spectroscopy, thermogravimetric analysis with Fourier transform infrared spectroscopy (TGA/FT-IR) and other analysis, including NMR, and Py-GC-MS. Consequently, the thermal degradation behaviours of the copolymers were determined through kinetic analysis.

2. Experimental details

2.1. Materials

The materials and detail preparation of the synthesis of PMEPP and MEPP/MMA copolymers have been described elsewhere [15,16].

* Corresponding author. Tel.: +886 6 2757575x62643.
E-mail addresses: n3894126@mail.ncku.edu.tw (W.-J. Chou), yokoi@gwip.com.tw (G.-A. Wang), ccwang@mail.stut.edu.tw (C.-C. Wang), ccy7@ccmail.ncku.edu.tw (C.-Y. Chen).

0032-3861/$ – see front matter Crown Copyright © 2009 Published by Elsevier Ltd. All rights reserved.
doi:10.1016/j.polymer.2009.08.037

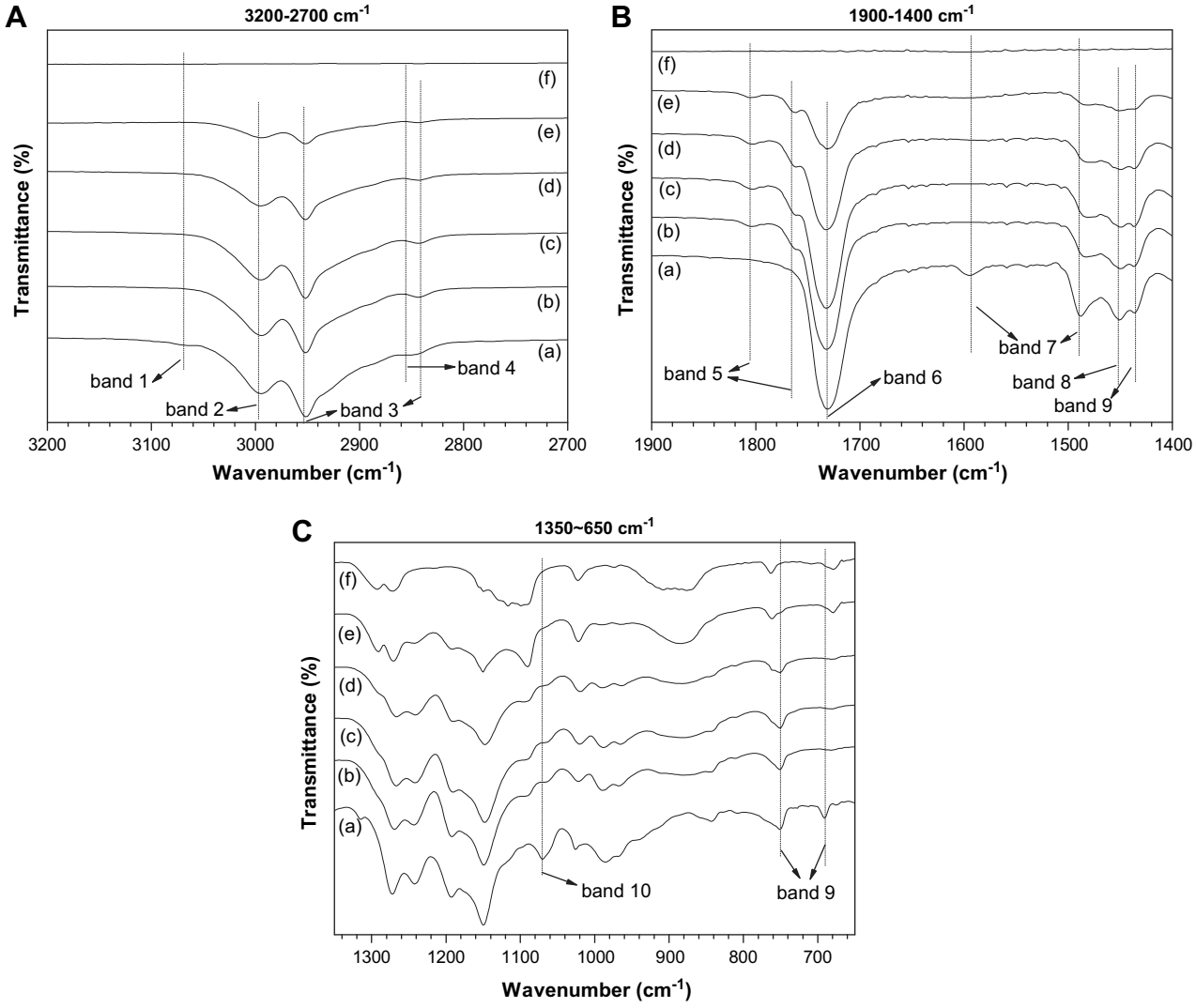

Fig. 1. FT-IR spectra of condensed-phase products at various temperatures during the thermal degradation of PMMA20. (a) Room temperature, (b) 250, (c) 300, (d) 330, (e) 360, (f) 400 °C.

2.2. Characterisations and measurements

Thermogravimetric analysis (TGA) was performed using a Perkin–Elmer TGA-7. Fifteen-milligram samples were heated at a heating rate of 20 °C min^{-1} under a nitrogen and air purge (70 mL min^{-1}). Each TGA experiment for the MEPP/MMA copolymers was repeated at least three times, with a typical temperature error of approximately ±1 °C. Approximately 2 g of MEPP/MMA was heated by a NEYTECH Qex 94-94-400 furnace at a 1 °C min^{-1} heating rate with air purging (70 mL min^{-1}) to 200 °C and was then held isothermally for 10 min to obtain the condensed-phase products at 200 °C. The condensed-phase product for the other temperature was obtained by the same procedure. Fourier transform infrared (FT-IR) spectra of these products were recorded on samples pressed into KBr disks using a Bio-Rad FTS-40A FT-IR spectrometer. Spectra in the optical range of 400–4000 cm^{-1} were obtained through the averaging of 64 scans at a resolution of 4 cm^{-1}. TGA/FT-IR studies were carried out using a TA TGA-Q50 thermogravimetric analyser that was interfaced to a Varian 2000 FT-IR spectrometer. The solid-state ^{31}P and ^{13}C magic angle spinning (^{31}P and ^{13}C MAS NMR) spectra were recorded with a Bruker AVANCE-400 solid-state NMR spectrometer. A pyrolysis gas chromatography/mass spectrometer (Py-GC/MS) was employed to achieve fast pyrolysis of sawdust and on-line analysis of the pyrolysis vapors with a Finnigan MD-800 GC/MS/JAI JHP-3S pyrolyser.

Table 1
The summary of the IR characteristic peaks during the thermal degradation of the PMMA20 condensed products.

Band No.	Wave number (cm^{-1})	Description
Band 1	3069	C–H stretching of aromatic
Band 2	2990	CH_3 asymmetric stretching of methyl group
Band 3	2950,2841	Symmetric and asymmetric stretching of CH_2
Band 4	2852	CH_2 stretching of P–O–P
Band 5	1805,1762	Ester stretching
Band 6	1728	C=O stretching of ester
Band 7	1594,1488	C=C stretching of aromatic
Band 8	1465	CH_2 bending
Band 9	1445	CH_3 asymmetric bending of methyl group
Band 10	1072	P–O–P stretching
Band 11	765,690	Out of plane bending of aromatic C–H

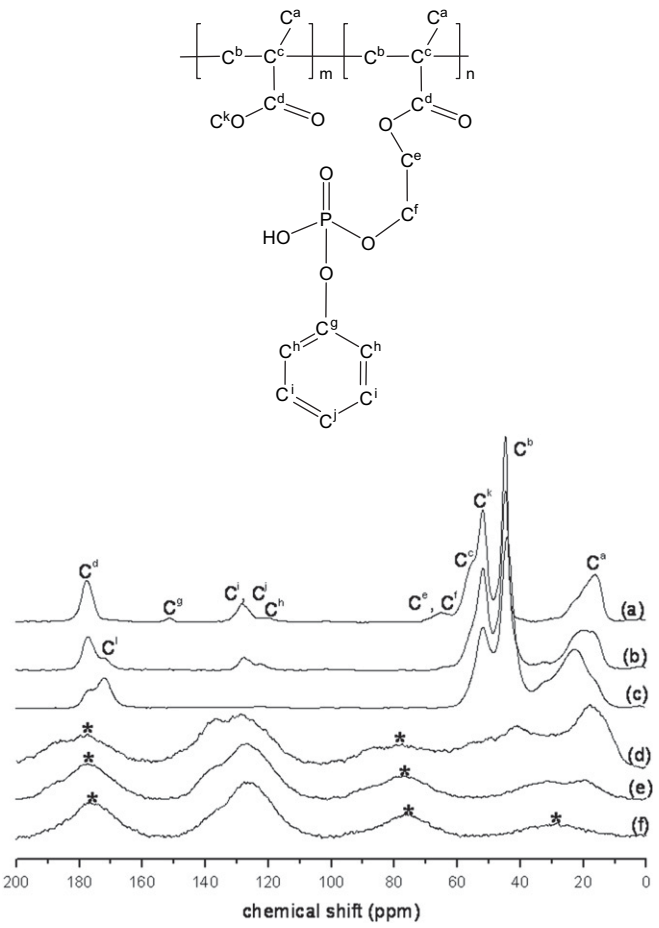

Fig. 2. ^{13}C solid-state NMR spectra of condensed-phase products at various temperatures during the thermal degradation of PMMA20. (a) Room temperature, (b) 250, (c) 300, (d) 400, (e) 500, (f) 600 °C.

3. Results and discussion

3.1. Characteristics of condensed-phase products

The condensed-phase products were characterised in order to investigate the thermal degradation mechanism of the 2-methacryloxyethyl phenyl phosphate (MEPP) and MEPP/methyl methacrylate (MEPP/MMA) copolymer. The data of those copolymers gave similar results hence, only the results for PMMA20 are discussed here. The condensed-phase products of PMMA20 were characterised by FT-IR, as shown in Fig. 1(A)–(C). The characteristic peaks in the spectrum in Fig. 1(A) can be assigned as follows: 3069 cm^{-1} (stretching vibration of aromatic C–H, band 1) [17–19], 2990 cm^{-1} (asymmetrical stretching vibration of methyl methacrylate CH_3, band 2), 2950 cm^{-1} and 2418 cm^{-1} (asymmetrical and symmetrical stretching of CH_2, band 3) [20] and 2852 cm^{-1} (stretching vibrations of CH_2 in the P-O-C aliphatic structure, band 4). The intensity of band 1 decreases with temperature and no visible changes can be observed beyond 250 °C, which may be caused by the unstable P–O–C aromatic structure of the copolymer PMMA20.In addition, the intensities of band 3 decreased with temperature from 250 °C to 400 °C and then vanished beyond 400 °C. These results can be attributed to the MMA chain degradated and can be further proved by the following data from the TGA/FT-IR in Fig. 5. The band 4 almost disappeared at 250 °C, which can be explained by the unstable P–O–C aliphatic structure breaking up during the thermal degradation of PMMA20.

In Fig. 1(B), band 6 at 1728 cm^{-1} was assigned to the stretching vibration of the ester group, C=O [19,21,22] and new peaks appeared at 1805 cm^{-1} and 1762 cm^{-1} (band 5) [20,21]. The peak at 1594 cm^{-1} and 1488 cm^{-1} are associated with stretching vibration of aromatic C=C (band 7) [19,20,23] and the band 8 at 1465 cm^{-1} was assigned to the CH_2 bending vibration. The asymmetrical bending vibration of methyl methacrylate CH_3 occurred at 1445 cm^{-1} (band 9). The intensity of band 5 increased with temperature from 250 °C to 300 °C, and the maximum value occurred at 300 °C. Beyond 300 °C, the intensity of band 5 began to decrease and disappeared at 400 °C. All of the changes in band 5 may be explained as follows. The ester structure of PMEPP started to transfer into a carbonic anhydride structure at 300 °C, leading to a simultaneous decrease in the intensity of band 6 and formation of band 5 [20,21]. In addition, the intensities of band 3 and band 8 decreased with temperature from 250 °C to 400 °C and then vanished beyond 400 °C. These results are attributed to the MMA chain degradated and can be further supported by the following data from the TGA/FT-IR.

In Fig. 1(C), the peaks at 765 cm^{-1} and 690 cm^{-1}were assigned as out of plane bending vibration of aromatic C–H (band 11) [20,24–27] and band 10 (1072 cm^{-1}) are assigned to the stretching vibrations of the P–O–C aliphatic structure. Bands 4 and 10 almost disappeared at 250 °C, which can be explained by the unstable

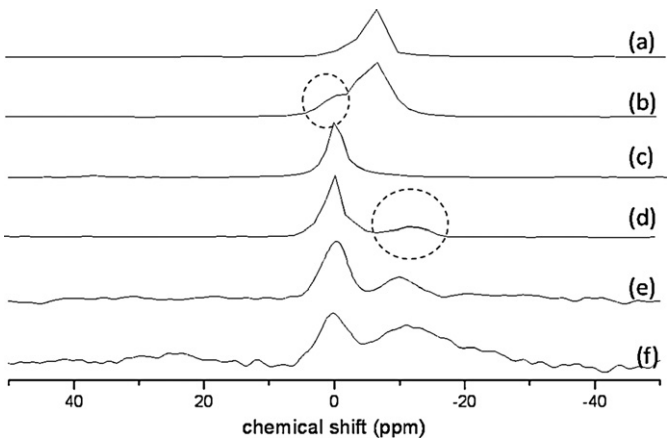

Fig. 3. ^{31}P solid-state NMR spectra of condensed-phase products at various temperatures during the thermal degradation of PMMA20. (a) Room temperature, (b) 230, (c) 250, (d) 330, (e) 400, (f) 600 °C.

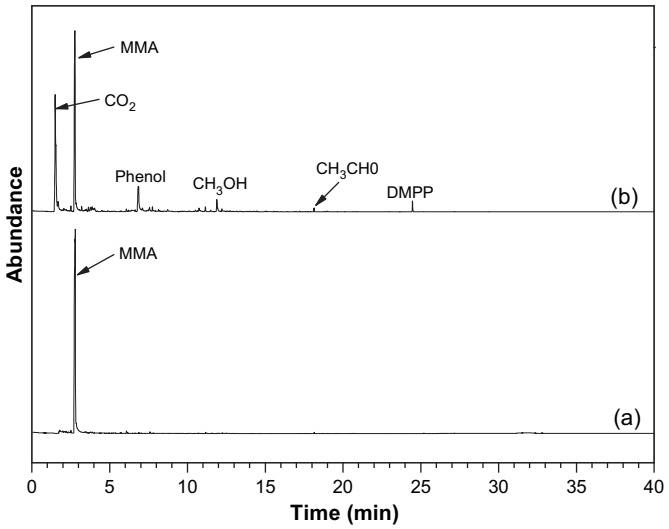

Fig. 4. Py-GC/Mass spectra of (a) PMMA and (b) PMMA20.

P–O–P aliphatic structure breaking up during the thermal degradation of PMMA20. The intensity of band 11 keeps constant after 250 °C, which is contributed from the thermal cracking of unstable P–O–C aromatic structure of the copolymer PMMA20. Many new peaks are appeared in Fig. 5(C), including peaks at 1292 cm^{-1}, 1273 cm^{-1}, 1150 cm^{-1}, 1023 cm^{-1}, 1089 cm^{-1}, 890 cm^{-1}, 760 cm^{-1}, and 679 cm^{-1} at 250 °C, and the intensities of those peaks increase with temperature. This shows that the remnants of the P–O–P and P–O–Φ complex structures, where Φ represents the graphite-like polynuclear aromatic structure [28–30], were formed during the thermal degradation of this copolymer (PMMA20) [27]. Zhu and Shi [27] developed phosphorus-containing homopolymer by UV polymerisation of methacrylate phosphate (MAP), showing the same results of formation of P–O–P and P–O–Φ complex structures during the thermal degradation of this homopolymer. All of the bands mentioned above are summarised in Table 1.

The condensed-phase analysis for the PMMA20 copolymer was carried out by solid-state NMR. Fig. 2 displays the ^{13}C MAS NMR spectra of the condensed-phase products at various temperatures. In Fig. 2(b), the signals of C^g, C^e, and C^f disappear, and a new signal (C^l) increases at 172.5 pm, which reveals that the unstable P–O–C structure in the MEPP unit cracked at 250 °C and that the carbonic anhydride [20,21] and carboxylic structures formed simultaneously [21]. The intensity of the C^l signal increased and the formation of the carbonic anhydride structure was continuous at 300 °C. However, the signals of C^l and C^d almost disappeared at 400 °C. The signals of the methyl and aromatic/olefinic groups were in the range of 10–30 ppm and 110–150 ppm, respectively. The results imply that the aromatic/olefinic complex structure is generated during ester structure decomposition. The signals in the range of 110 to 150 ppm increased from 400 °C to 600 °C, and the peaks in the range of 10–30 ppm decayed rapidly at 600 °C. Finally, as shown in Fig. 2(f), the signals in the range of 110–150 ppm appeared at 600 °C and were attributed to the conversion of the aromatic/olefinic groups into various kinds of P–O–P and P–O–Φ complex structures during the thermal degradation of PMEPP20, resulting in a graphite-like polynuclear aromatic structure [31,32].

The ^{31}P solid-state NMR spectra of PMMA20 thermal degradation at different temperatures are shown in Fig. 3. A new peak appeared ($\delta = 0$ ppm) at 230 °C, which was attributed to the

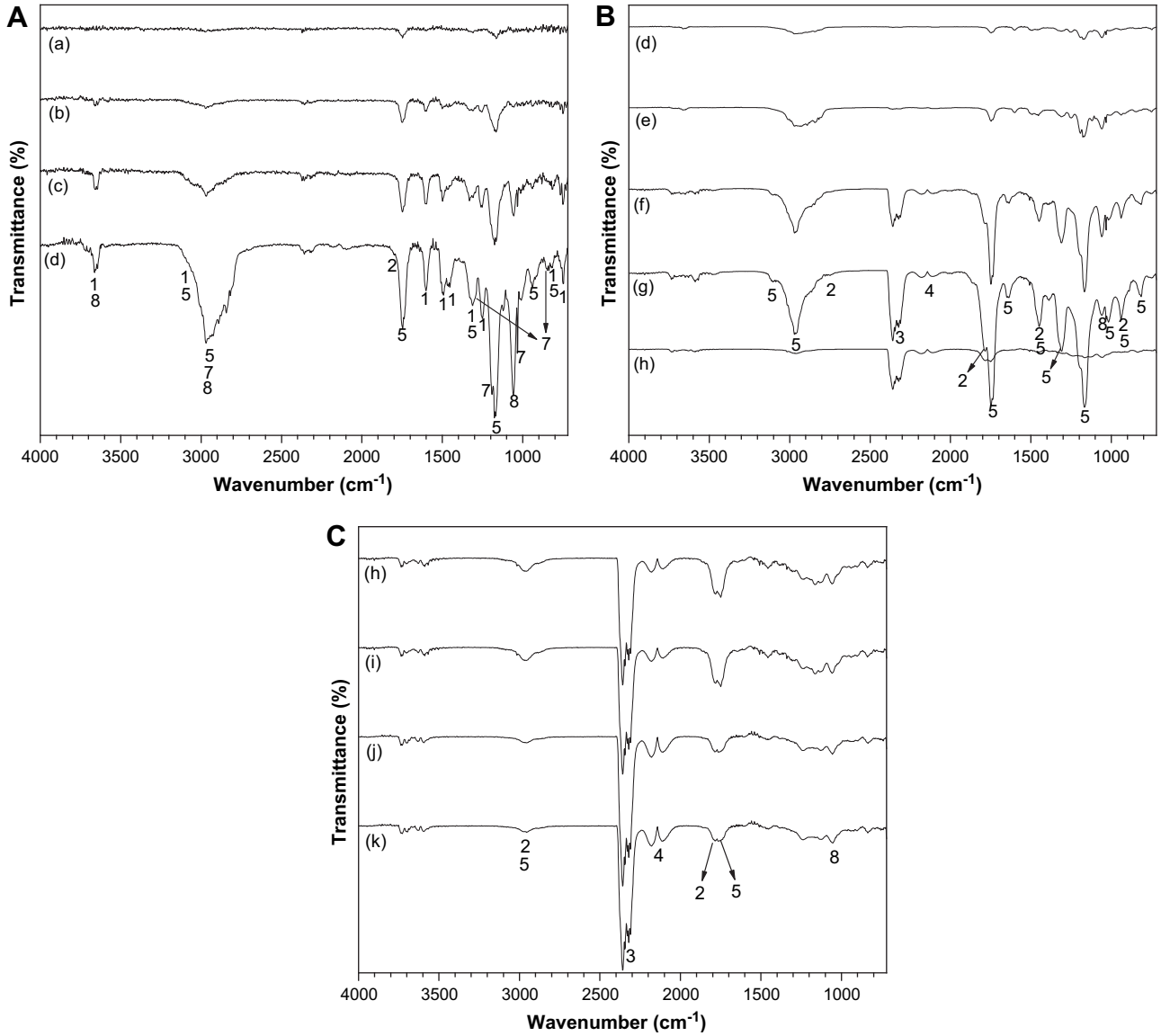

Fig. 5. FT-IR spectra of volatilized products at various temperatures during the thermal degradation of PMMA20. (a) 250, (b) 290, (c) 330, (d) 375, (e) 395, (f) 415, (g) 433, (h) 455, (i) 485, (j) 525, (k) 565 °C (1: phenol 2: aldehyde 3: CO_2 4: CO 5: MMA 6: water 7: phosphate 8: alcohol.).

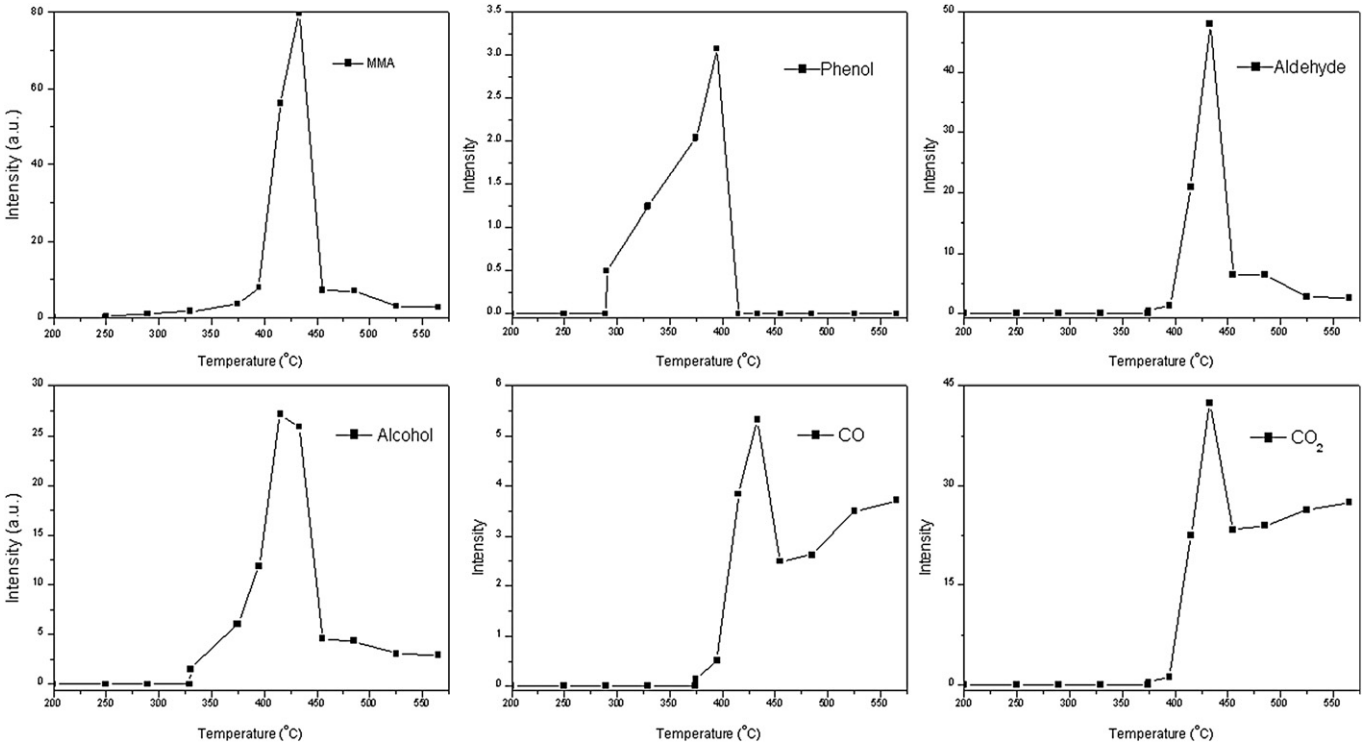

Fig. 6. Relationship between the intensity of the characteristic peak and temperature for MMA, phenol, CO, CO_2, and alcohol.

carbonic anhydride or polyphosphoric acid structures that were formed during the thermal degradation of the MEPP unit. As the temperature increased to 250 °C, the original peak of phosphorus nearly disappeared. In other words, the MEPP unit was completely degraded confirming the results from the FT-IR spectra (Fig. 1). In addition to the original signal at 0 ppm, a new broad peak appeared between $\delta = -8$ ppm and $\delta = -20$ ppm at temperatures above 330 °C. Moreover, the intensity of the new peak increased with temperature, and the P–O–P and P–O–Φ complex structures were formed, Ebdon et al. had the similar results [21].

The summary of the results depicted in Figs. 1–3 specifies that the thermal degradation of MEPP/MMA copolymers can be approximately separated into six processes: the scission of the unstable P–O–P aromatic and aliphatic structure, the decomposition of the MMA unit, the decomposition of the ester group occurring with the formation of the carbonic anhydride structure,

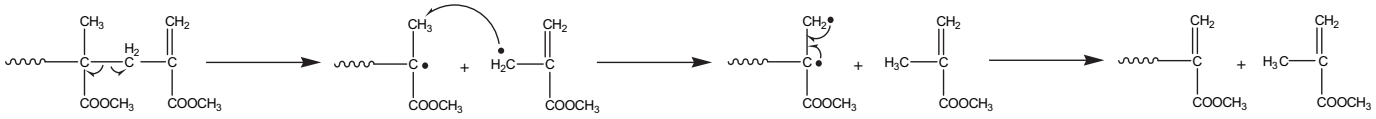

(A-1a)

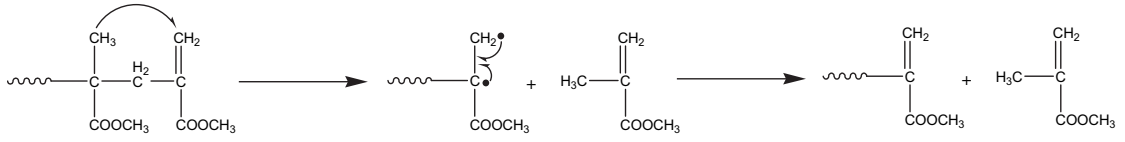

(A-1b)

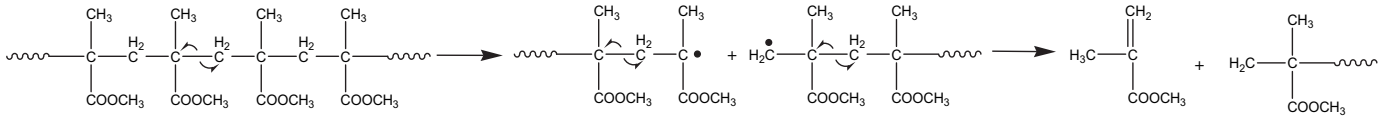

(A-2)

Scheme 1.

the decomposition of the carbonic anhydride structure, the scission of the methyl group, and the formation of the P–O–P and P–O–Φ complex structures.

3.2. Characteristics of volatilized products

During the PMMA decomposition, the release products were characterised by Py-GC/Mass. The Py-GC/Mass spectrum is shown in Fig. 4 and contains only a peak for the MMA unit. In other words, the MMA monomer was the main phase product for the thermal degradation of PMMA [33]. This reveals that the thermal degradation of PMMA was a depolymerisation reaction. The release of thermal degradation products was examined by TGA-FTIR at different temperatures and is displayed in Figs. 5 and 6. The PMMA20 copolymer began to decompose at temperatures higher than 250 °C, which resulted in mass loss.

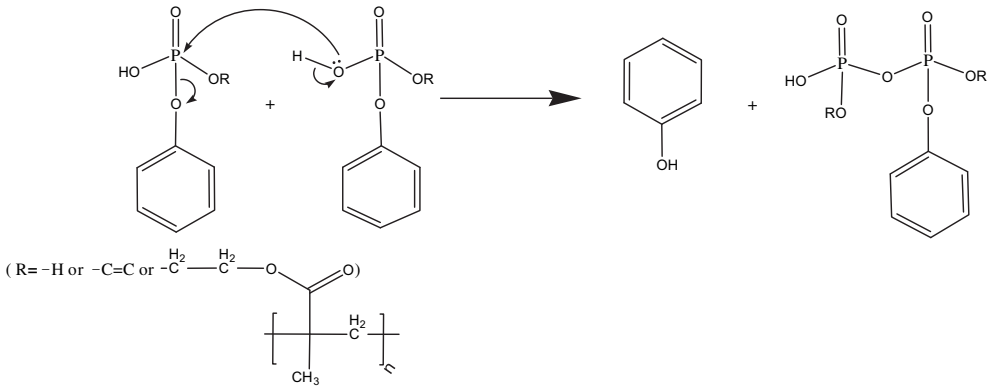

(B-1a) Scission of P-O-C aromatic

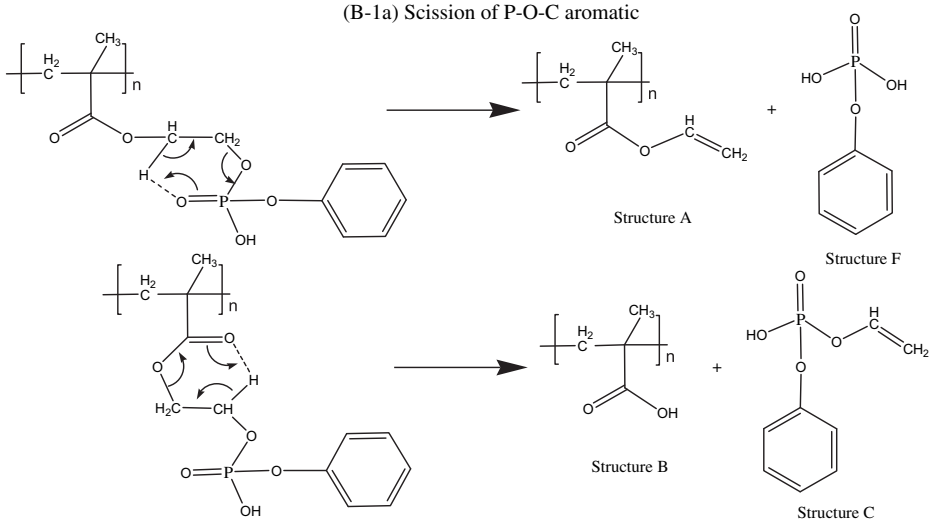

(B-1b) Scission of P-O-C aliphatic

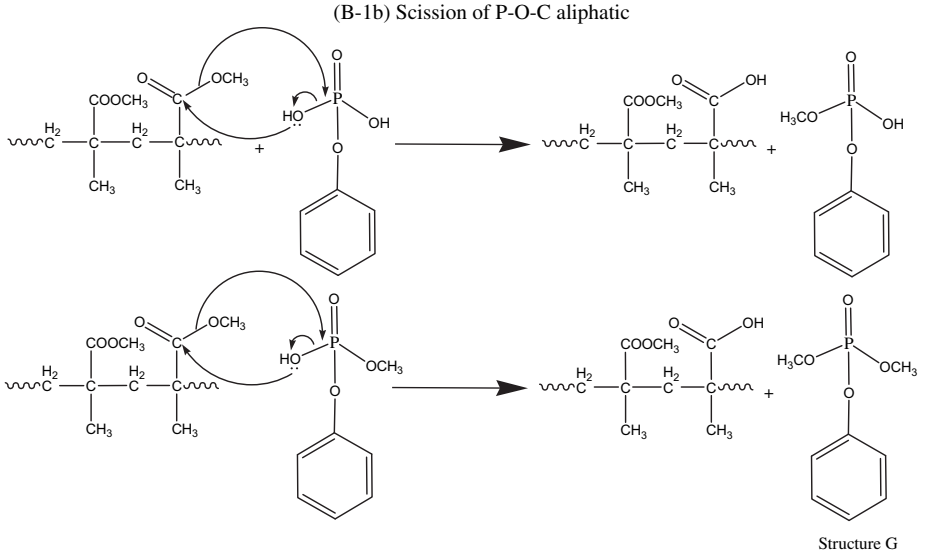

(B-1c) Elimination of phosphate

Scheme 2.

The following characteristic bands were observed: MMA (2960, 1740, 1640, 1452, 1309, 1166, 1019, and 934 cm^{-1}) at 250 °C, phenol (3655, 3057, 1602, 1499, 1260, 1184, 748 cm^{-1}) at 290 °C and alcohol (3675, 2969, 2921, 1406, 1250, 1065, and 590 cm^{-1}) at 330 °C. At temperatures greater than 375 °C, the peaks of aldehyde (3675, 2969, 2921, 1406, 1250, 1065, and 1184 cm^{-1}), CO (2197 and 2110 cm^{-1}), and CO_2 (2359 and 2322 cm^{-1}) were detected. The signals of water did not appear during the decomposition of the PMMA20 copolymer (Fig. 5). In addition, apparent peaks of phosphate were observed during the decomposition of the PMMA20 copolymer from 330 °C to 433 °C.

In order to understand the changes occurring in these formative products, the relationships between the intensity of the characteristic peak and the temperature of the release products (MMA, phenol, aldehyde, alcohol, CO, and CO_2) of PMMA20 copolymer decomposition are summarised in Table 1. It can be seen that the formative temperature of MMA can be approximately forced to 375–525 °C, though a small amount of MMA was detected from 250 °C to 375 °C. In other words, the ratio of MMA decomposition by unsaturated end-group initial scissions was too low, and the thermal degradation of most MMA units initially took place along the main chain. The signal of phenol was observed at 290 °C and increased with temperature, reaching a maximum at 390 °C. Beyond 390 °C, the intensity of phenol rapidly decreased and almost disappeared by 415 °C. Furthermore, the peak corresponding to alcohol increased with temperature up to 450 °C but quickly decreased beyond 450 °C. At higher temperatures, up to 565 °C the weak signal of alcohol still exists. The peak for aldehyde showed a behavior similar to that of alcohol.

Finally, the formative temperature of CO or CO_2 can be divided into two regions: 375–450 °C and 450–650 °C. These ranges may result from the decomposition of the anhydride structure and the further oxidation of char, respectively. From the results shown in Figs. 4(b) and 5, we can conclude that the volatilized products for the thermal degradation of PMMA20 are MMA, CO_2, phenol, aldehyde, alcohol, and phosphate (DMPP).

However, the volatilized products that are formed during the thermal degradation of PMMA20, including MMA, phenol,

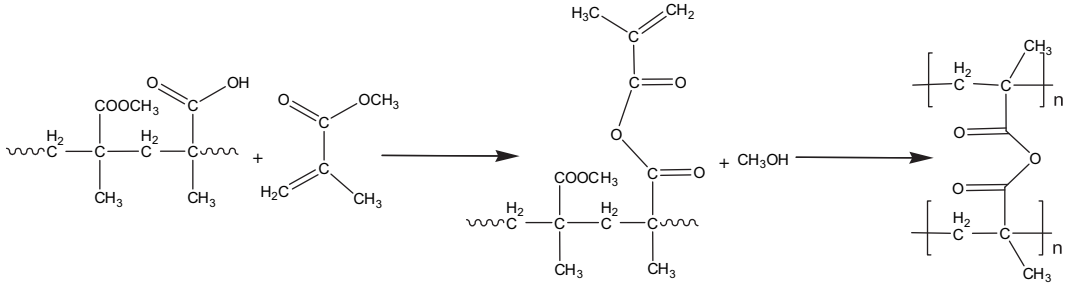

(B-2a) Capture of MMA

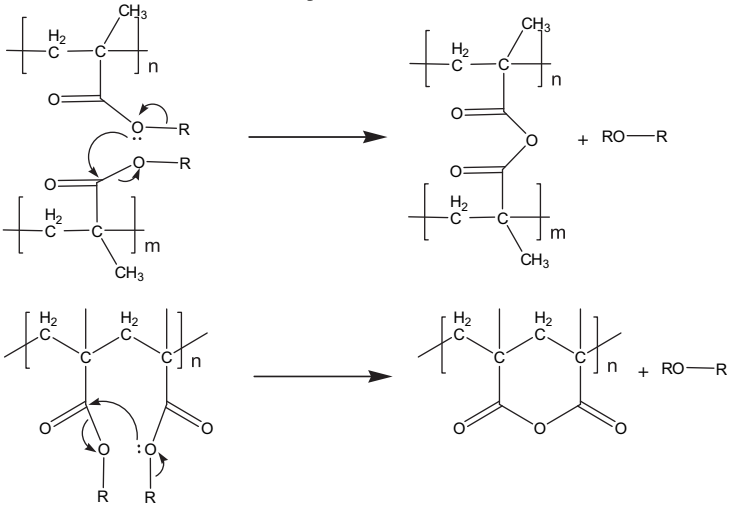

(R= -H or -CH_3 or -$CH{=}CH_2$)

(B-2b) Formations of intra-or intermolecular carbonic anhydride structure

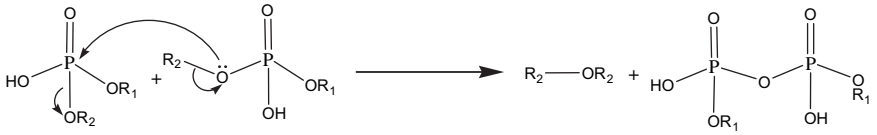

(R_1= - P=O)

(R_2= -H or -CH_3 or -$CH{=}CH_2$)

(B-2c) Formations of intermolecular phosphoric anhydride structure

Scheme 3.

aldehyde, CO, and CO_2, appeared at higher temperatures than those of PMMA and PMEPP. This reveals that the incorporation of MEPP caused MEPP/MMA copolymers to exhibit better thermal stability. Cochez et al. obtained similar results for phosphonate/MMA copolymers with flame retardant [34].

3.3. Possible mechanisms for the thermal degradation of the MEPP/MMA copolymer

By combining the analytical results of the condensed phase obtained with FI-IR, ^{13}C NMR, ^{31}P NMR, the volatilized products obtained by TGA/FT-IR and Py-GC/Mass, and the previous literature for thermal degradation of PMMA [35,36] and PMEPP [2,4,37], we propose possible mechanisms for the thermal degradation of PMEPP. We divide these into two parallel reactions: (A) scissions of the MMA unit and (B) scissions of the MEPP structure, as shown from Schemes 1–4. According to the literature [35,36,38], the first reaction, scission of the MMA unit, involves unsaturated end-group fragmentation, including the β-scission reaction (Scheme 1, A-1a) and the end-scission reaction (Scheme 1, A-1b). Next, as the temperature increases, the thermal degradation of the MMA unit takes place along the main chain, as shown in Scheme 1 (A-2).

Based on the above results, the scissions of the MEPP structure may be divided into five steps, occurring in sequence as the temperature increases, the similar results have reported in our previous research [15]. Apparently, the first step involves the scissions of the least stable P–O–P aromatic and aliphatic structures. In other word, the thermal degradation of PMEPP takes place initially along the side chain. The scission of the P–O–P aromatic structure by a condensation reaction results in the elimination of phenol (Scheme 2, B-1a). The scission of the P–O–P aliphatic structure by a rearrangement of the intramolecular structure forms the possible structures A, B, C, and F (Scheme 2, B-1b). The formation of structure F can occur by a transesterification reaction with the MMA unit of the MEPP/MMA copolymer and can cause the elimination of phosphate and the formation of structure B (Scheme 2, B-1c).

The formation of the phosphoric and carbonic anhydride structures is the second step. The formation of the intramolecular phosphoric anhydride structures by the condensation reaction between structure B and the MMA of the MEPP/MMA copolymer cause the elimination of alcohol (Scheme 3, B-2a). Structures B and A undergo a condensation reaction forming the intra- or intermolecular carbonic anhydride structure, with the elimination of aldehyde and alcohol (Scheme 3, B-2b). In addition, structure C and phosphoric acid precede the condensation reaction by constructing intramolecular phosphoric anhydride, with the elimination of aldehyde (Scheme 3, B-2c). In this study, the peak for water did not appear during the thermal degradation of the MEPP/MMA

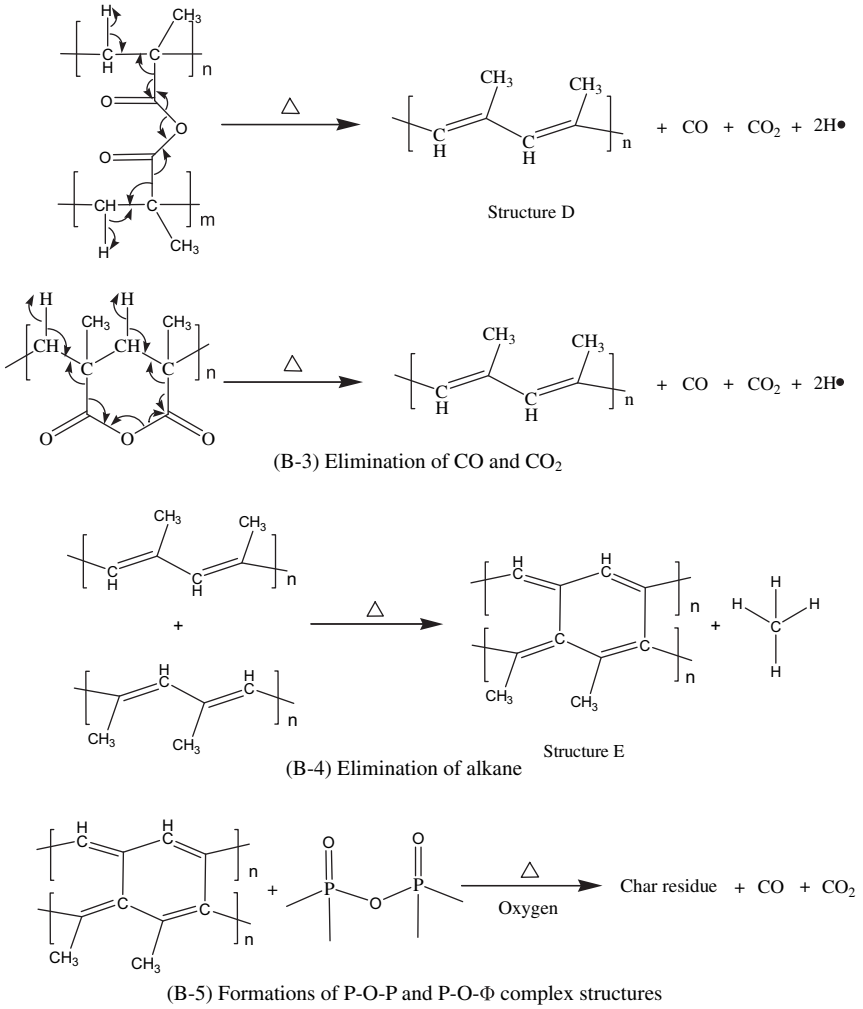

Scheme 4.

copolymer and was replaced by that of alcohol. This may be attributed to the fact that the amount of MMA is higher than that of MEPP during the thermal degradation of the copolymer and the probability of alcohol elimination is stronger than that of water elimination. Therefore, the signal of water did not appear during the analysis of the release gas of the copolymer.

During the thermal degradation of PMEEP, that the formations of carbonic anhydride structures further decomposed are classified as the third portion. The decompositions lead to the elimination of CO_2 and CO as well as the formation of structure D (Scheme 4, B-3). We can observe the change arising from methyl scission at high temperatures by ^{13}C NMR analysis. The fourth step involves a series of intra- and intermolecular Diels–Alder reactions between adjacent unsaturated sequences of structure D, accompanied by the elimination of alkane and the formation of structure E (Scheme 4, B-4). In comparison with PMEPP, the amount of structure D was lower during the thermal degradation of the MEPP/MMA copolymer with a low MEPP content. Hence, it was difficult to observe the signal of the alkane elimination caused by the Diels–Alder reaction. The last step involves the formation of a char residue with P–O–P and P–O–Φ complex structures. The char residue is formed from the oxidation of structure E, simultaneously linking structure E with other P–O–P structures at high temperatures (Scheme 4, B-5).

4. Conclusion

MEPP/MMA copolymers containing various amounts of MEPP were prepared by a two-stage bulk polymerisation process. The results of the analysis of condensed-phase products and volatilized products can be separated into four conclusions: (1) The MEPP in the PMMA enhances flame retardance and delays the elimination of the MMA unit. (2) Due to the inclusion of MEPP, a new mechanism was developed, and the volatilized products for the thermal degradation of MEPP/MMA copolymer, including CO, CO_2, and char residue, reduced the concentrations of combustible gas and oxygen. (3) The decomposition of the carbonic anhydride structure and the formation of P–O–P and P–O–Φ complex structures cover the burning substances and decrease the transmission of oxygen, heat, and active gas.

Acknowledgements

The authors would like to thank the Ministry of Economic Affairs of the Republic of China for financial support of this research under contract no. TDPA 97-EC-17-A-05-S1-0014 and the National Science Council of the Republic of China for the instruments and partial financial support of this research (NSC97-2221-E-006-027-MY3).

References

[1] Jellinek HHG, Clark JE. Canadian Journal of Chemistry 1963;41(2):355–62.
[2] Lehmann FA, Brauer GM. Analytical Chemistry 1961;33(6):673–6.
[3] Robert Simha LAW, Blatz PJ. Journal of Polymer Science 1950;5(5):615–32.
[4] Taylor HS, Tobolsky AV. Journal of the American Chemical Society 1945;67(12):2063–7.
[5] Laachachi A, Cochez M, Ferriol M, Leroy E, Lopez Cuesta JM, Oget N. Polymer Degradation and Stability 2004;85(1):641–6.
[6] Zhang J, Zhang Z, Tang Z, Wang T. Ceramics International 2004;30(2):225–8.
[7] Reghunadhan CP, Nair GC, Brossas J. Journal of Polymer Science, Part A: Polymer Chemistry 1988;26(7):1791–807.
[8] Reghunadhan Nair CP, Clouet G. Polymer 1988;29(10):1909–17.
[9] Reghunadhan Nair CP, Clouet G. European Polymer Journal 1989;25(3):251–7.
[10] Reghunadhan Nair CP, Clouet G, Guilbert Y. Polymer Degradation and Stability 1989;26(4):305–31.
[11] Price D, Pyrah K, Hull TR, Milnes GJ, Ebdon JR, Hunt BJ, et al. Polymer Degradation and Stability 2002;77(2):227–33.
[12] Price D, Pyrah K, Hull TR, Milnes GJ, Ebdon JR, Hunt BJ, et al. Polymer Degradation and Stability 2001;74(3):441–7.
[13] Chin-Ping Yang, Sheng-Sung Wang. Journal of Polymer Science, Part A: Polymer Chemistry 1989;27(11):3551–67.
[14] Wang G-A, Wang C-C, Chen C- Y. Polymer Degradation and Stability 2006;91(10):2443–50.
[15] Wang G-A, Cheng W-M, Tu Y-L, Wang C-C, Chen C-Y. Polymer Degradation and Stability 2006;91(12):3344–53.
[16] Wang G-A, Wang C-C, Chen C-Y. Polymer Degradation and Stability 2006;91(11):2683–90.
[17] Antony R, Pillai CKS. Journal of Applied Polymer Science 1993;49(12):2129–35.
[18] Leu TS, Wang CS. Journal of Applied Polymer Science 2004;92(1):410–7.
[19] Wang TL, Cho YL, Kuo PL. Journal of Applied Polymer Science 2001;82(2):343–57.
[20] Pavia DL, Lampman GM, Kriz GS. Introduction to spectroscopy: a guide for students of organic chemistry. 2nd ed. Orlando: Saunders; 1996.
[21] Ebdon JR, Hunt BJ, Joseph P, Konkel CS, Price D, Pyrah K, et al. Polymer Degradation and Stability 2000;70(3):425–36.
[22] Price D, Pyrah K, Hull TR, Milnes GJ, Wooley WD, Ebdon JR, et al. Polymer International 2000;49(10):1164–8.
[23] Liaw DJ, Shen WC. Angewandte Makromolekulare Chemie 1994;214:169–78.
[24] Bourbigot S, Bras M, Delobel R, Tremillom J. Journal of Chemical Society Faraday Transactions 1996;92:3435.
[25] Ferriol M, Gentilhomme A, Cochez M, Oget N, Mieloszynski JL. Polymer Degradation and Stability 2003;79(2):271–81.
[26] Lyon RE. Thermochimica Acta 1997;297(1-2):117–24.
[27] Zhu SW, Shi WF. Polymer Degradation and Stability 2003;80(2):217–22.
[28] Bugajny M, Bourbigot S, Le Bras M, Delobel R. Polymer International 1999;48(4):264–70.
[29] Hsiue GH, Wei HF, Shiao SJ, Kuo WJ, Sha YA. Polymer Degradation and Stability 2001;73(2):309–18.
[30] Nyquist RA. Applied Spectroscopy 1957;11(4):161–4.
[31] Cody GD, Alexander CMO. Geochimica Et Cosmochimica Acta 2005;69(4):1085–97.
[32] Freitas JCC, Emmerich FG, Cernicchiaro GRC, Sampaio LC, Bonagamba TJ. Solid State Nuclear Magnetic Resonance 2001;20(1–2):61–73.
[33] McNeill IC. Comprehensive polymer science. Oxford; 1989.
[34] Cochez M, Ferriol M, Weber JV, Chaudron P, Oget N, Mieloszynski JL. Polymer Degradation and Stability 2000;70(3):455–62.
[35] Jellinek HH, Luh MD. Journal of Physical Chemistry 1966;70(11):3672.
[36] Jellinek HH, Luh MD. Makromolekulare Chemie-Macromolecular Chemistry and Physics 1968(Jun);115:89.
[37] Barlow A, Lehrle RS, Robb JC, Sunderla D. Polymer 1967;8(10):537.
[38] Jellinek HH, Kachi H. Journal of Polymer Science Part C-Polymer Symposium 1968;(23PC):87.